

Energy-Saving Adaptive Robust Motion Control of Single-Rod Hydraulic Cylinders with Programmable Valves¹

Bin Yao⁺ Chris DeBoer

School of Mechanical Engineering
Purdue University, West Lafayette, IN 47907, USA
byao@ecn.purdue.edu

Abstract

This paper studies the energy-saving adaptive robust motion control of a single-rod hydraulic cylinder through the use of programmable valves. The programmable valve used in this study is a unique combination of five proportional cartridge valves connected in such a way that the meter-in and meter-out flows can be independently controlled by four of the valves as well as a true cross port flow controlled by the fifth valve. The programmable valve decouples the meter-in and meter-out flows which in turn allows tremendous control flexibility. Although at the expense of controller complexity, if well utilized, the added control flexibility can be used to significantly reduce the fluid power energy usage in a number of motion and loading conditions to meet the society's need for energy conservation while without sacrificing the achievable motion control accuracy. Such a coordinated control solution is provided in the paper, and is shown effective through both the simulation and experimental results in the likely operating conditions of a typical industrial backhoe loader arm.

1 Introduction

The control of an electro-hydraulic system is far from trivial, due to factors such as the highly nonlinear hydraulic dynamics, large parameter variations, and significant uncertain nonlinearities such as external disturbances, flow leakages and seal frictions [8, 10]. Traditionally, a typical four-way directional control valve (or a servo valve) is used for each cylinder [8, 10]. With such a hardware configuration, only one of the two cylinder states (i.e., pressures of the two chambers) is completely controllable and there exists a one-dimensional internal dynamics. Although the one-dimensional zero dynamics are shown to be stable [3], it cannot be modified by any trajectory tracking control strategy. The result is that while high performance output trajectory tracking can be attained, simultaneous high levels of energy savings cannot.

¹The project is supported in part by the National Science Foundation under the CAREER grant CMS-9734345. The fund from the Purdue Electro-Hydraulic Research Center supported by the Caterpillar Inc. and the donation of cartridge valves by Vickers Inc. for setting up the programmable valves used in the experiments are gracefully acknowledged.

The uncontrollable state is due to the fact that the meter-in and meter-out orifices are mechanically linked together in a typical directional control valve. This is a fundamental drawback of typical four-way directional control valves. If this link were to be broken the flexibility of the valve control could be drastically increased, making the way for significant improvements in energy savings [6].

Although not so much in academic community, there have been substantial amount of activities in industry on breaking the mechanical linkage between the meter-in and meter-out orifices, as attested by various US patents [6, 1, 7, 5]. Those hardware configurations [6, 1, 7, 5] provide the possibility of independent control of each meter-in and meter-out ports. However, it should be realized that, to be able to achieve significant energy savings, it is necessary to take the advantage of regeneration flow. Regeneration flow [1, 5] is the fluid pumped from one chamber to the other chamber using the energy of the external load, in which little pump energy is needed. The four valve metering unit proposed in [6, 1, 7, 5] enables the use of regeneration flow to certain degree but not to the fullest extent possible [1] as a truly controlled cross port flow is not available.

The novel valve configuration used in this study takes the advantage of four-valve poppet-type configuration [1, 2] and makes the addition of an additional valve to enable a true cross port flow that is fully controllable. With such a novel configuration, not only meter-in/meter-out can be fully independently controlled for precise output trajectory tracking and for keeping pressures at suitable levels to achieve certain amount of energy saving, but also the cross port regenerative flow can be precisely controlled to keep total pump (or active) flow energy usage minimum for maximum energy savings. The proposed programmable valve configuration is given in Fig. 1.

This study is a preliminary work in investigating the most effective and efficient use of the proposed novel programmable valve (Fig.1) in achieving the dual objectives of high performance motion tracking and energy savings. The programmable valve is implemented on a robot arm modelled after a typical industrial backhoe shown in Fig. 2.

2 Problem Formulation and Dynamic Model

To illustrate the uniqueness and the application of the proposed programmable valves, the boom motion control of a three degree-of-freedom electro-hydraulic robot arm that was built to mimic the industrial backhoe or excavator arms in [10] is considered. The boom motion dynamics with other two joints fixed can be described by [4].

$$(J_c + m_L \ell_e^2) \ddot{q}_2 + G_c(q_2) + m_L g \ell_g = \frac{\partial x_L}{\partial q_2} (P_1 A_1 - P_2 A_2) + T_d \quad (1)$$

where q_2 represents the boom joint angle, J_c is the moment of inertia of the boom without payload, m_L represents the mass of the unknown payload, G_c is the gravitational force of the boom without payload, x_L represents the boom hydraulic cylinder displacement, P_1 and P_2 are the head and rod end pressures of the cylinder respectively, A_1 and A_2 are the head and rod end areas of the cylinder respectively, T_d represents the lumped disturbance torque including external disturbances and terms like the unmodelled friction torque. The specific forms of J_c , G_c , $\ell_g(q_2)$, and ℓ_e^2 are given in [4].

Assuming no cylinder leakage [8], the cylinder equations can be written as,

$$\begin{aligned} \frac{V_1(x_L)}{\beta_e} \dot{P}_1 &= -A_1 \dot{x}_L + Q_1 = -A_1 \frac{\partial x_L}{\partial q_2} \dot{q}_2 + Q_1 \\ \frac{V_2(x_L)}{\beta_e} \dot{P}_2 &= A_2 \dot{x}_L - Q_2 = A_2 \frac{\partial x_L}{\partial q_2} \dot{q}_2 - Q_2 \end{aligned} \quad (2)$$

where $V_1(x_L) = V_{h1} + A_1 x_L$ and $V_2(x_L) = V_{h2} - A_2 x_L$ are the total cylinder volumes of the head and rod end respectively, V_{h1} and V_{h2} are the initial control volumes when $x_L = 0$, β_e is the effective bulk modulus. Q_1 and Q_2 are the supply and return flows respectively.

For the programmable valve in Fig. 1, Q_1 and Q_2 are given by,

$$Q_1 = Q_{v2} - Q_{v1} - Q_{v3}, \quad Q_2 = -Q_{v3} - Q_{v4} + Q_{v5} \quad (3)$$

where the orifice flows Q_{vi} can be described by

$$\begin{aligned} Q_{v1} &= f_{v1}(\Delta P_{v1}, x_{v1}) & \Delta P_{v1} &= P_1 - P_t \\ Q_{v2} &= f_{v2}(\Delta P_{v2}, x_{v2}) & \Delta P_{v2} &= P_s - P_1 \\ Q_{v3} &= f_{v3}(\Delta P_{v3}, x_{v3}) & \Delta P_{v3} &= P_1 - P_2 \\ Q_{v4} &= f_{v4}(\Delta P_{v4}, x_{v4}) & \Delta P_{v4} &= P_s - P_2 \\ Q_{v5} &= f_{v5}(\Delta P_{v5}, x_{v5}) & \Delta P_{v5} &= P_2 - P_t \end{aligned} \quad (4)$$

in which f_{vi} is the nonlinear orifice flow mapping as a function of the pressure drop, ΔP_{vi} , and the orifice opening, x_{vi} , of the i th cartridge valve. Neglecting valve dynamics, x_{vi} is related to the command valve voltage v_i by a known mapping, i.e., $x_{vi} = x_{vi}(v_i)$.

Due to the fact that the nonlinear flow mappings are very difficult to determine accurately, it is assumed that

$$Q_1 = Q_{1M} + \tilde{Q}_1, \quad Q_2 = Q_{2M} + \tilde{Q}_2 \quad (5)$$

where Q_{1M} and Q_{2M} represent the flows from the approximated valve mappings and \tilde{Q}_1 and \tilde{Q}_2 represent the modelling errors of the flow mappings. The effect of the flow modelling errors will be dealt with through robust feedback.

Given the desired motion trajectory $q_{2Ld}(t)$, the primary objective is to synthesize valve control voltages such that the output $y = q_2$ tracks $q_{2Ld}(t)$ as closely as possible in spite of various model uncertainties. The second objective is to minimize the overall energy loss.

3 Energy-Saving Adaptive Robust Controller Design

To meet the dual objectives of precise motion control and significant energy saving, the following general strategies are adopted: (i) the nonlinear model based adaptive robust control design [10, 3] is used to directly deal with the common difficulties in the precision control of electro-hydraulic systems – nonlinear dynamics, parameter variations, uncertain nonlinearities and the mismatched model uncertainties – to synthesize the desired load flow that is needed for precise motion control; and (ii) a nonlinear adaptive robust pressure controller is developed to handle the pressure control of the off-side chamber for energy saving purpose. The difficulties of pressure control, valve nonlinearities and coordinated control of five cartridge valves is accomplished through a task level and valve level controllers. Given the current situation, the task level controller determines the configurations of programmable valve that enable significant energy saving while without losing achievable motion control performance. The valve level controller uses a model based adaptive robust pressure controller for off-side pressure control and uses an adaptive robust motion controller for motion trajectory tracking. The valve level also makes use of pressure compensated inverse valve mappings to handle the effect of nonlinear valve flow mappings in order to provide the correct control flows to the two chambers of the cylinder.

3.1 Task Level: Valve Utilization

Let Q_{1d} and Q_{2d} be the desired control flows to the two chambers of the cylinder that are needed for both the precision motion tracking and maintaining the lowest possible cylinder chamber pressures to reduce the flow losses for energy saving. The task level of the controller determines how the five valves of the proposed programmable valve in Fig. 1 should be used in order to provide the required control flows Q_{1d} and Q_{2d} . Obviously, such a process is not unique due to the added flexibility of independently controlling each of these five valves. This subsection describes the six most popular configurations that have been proposed in hydraulic industry [1] and how these configurations are implemented on the proposed programmable valve set. The six configurations are the extend resistive, extend overrunning, extend overrunning regeneration, retract resistive, retract overrunning, and the retract overrunning regeneration as summarized below:

- **Extend Resistive**

The extend resistive mode is a standard operation in which the control command calls for the cylinder to be extended (i.e., $\dot{x}_L \geq 0$) with a resistive load (i.e., $F_{load} < 0$). In such a situation, valve 2 in Fig. 1 is used

to provide the control flow Q_{1d} to the head end chamber for precision motion control, and valve 5 to control the flow Q_{2d} to maintain a low pressure in the rod end chamber for energy saving. The remaining three valves are closed.

- **Extend Overrunning**

The extend overrunning mode is defined as when the cylinder is to be extended (i.e., $\dot{x}_L \geq 0$), with an overrunning load (i.e., $F_{load} > 0$). In this case, valve 5 is used to provide Q_{2d} to regulate the motion of the cylinder, and valve 2 to maintain a minimal head end pressure. The remaining three valves are closed.

- **Extend Overrunning Regeneration**

The extend overrunning regeneration mode is similar to the previous mode in that the cylinder is to be extended ($\dot{x}_L \geq 0$) under an overrunning load ($F_{load} > 0$) but with the additional requirement that $P_2 > P_1$ so that the external load is sufficient to pump fluid from the rod end of the cylinder into the head end of the cylinder through valve 3. This reduces the flow needed from the pump and saves energy dramatically. Flow from the pump is still needed due to the larger head end area. For such a case, valve 3 is used to control the cylinder motion and valve 2 to provide the additional flow needed to maintain the desired head end pressure.

- **Retract Resistive**

The retract resistive mode is a standard cylinder function in that the cylinder is to be retracted ($\dot{x}_L \leq 0$) under a resistive load ($F_{load} < 0$) as defined relative to the desired cylinder motion. Valve 4 is used to provide the control flow for motion control and valve 1 is used to maintain the head end pressure at a low level.

- **Retract Overrunning**

The retract overrunning mode is used in the situation that the cylinder is to be retracted ($\dot{x}_L \leq 0$) under an overrunning load ($F_{load} < 0$). In this mode, valve 1 is used to control the cylinder motion and valve 4 is used to regulate the rod end pressure.

- **Retract Overrunning Regeneration**

The retract overrunning regeneration mode occurs under the same conditions as the previous mode ($\dot{x}_L \leq 0$ and $F_{load} < 0$) but with the additional requirement that $P_1 > P_2$ to ensure that the external load is large enough to pump fluid from the head end chamber to the rod end chamber through valve 3. The excess flow due to the differing head and rod end areas is drained to the tank through valve 1. Valves 1 and 3 are used to regulate the head end pressure to control the cylinder motion. Valve 5 is completely opened to the tank as a preventative anti-cavitation measure to maintain the rod-end pressure at the minimum reference pressure for energy saving. The result is an extremely efficient mode that requires no pump flow.

3.2 Valve Level: ARC Pressure Controller Design

The pressure controller design is intended to regulate the pressure of the off-side of the cylinder. The working side is defined as the side critical to the motion of the cylinder and the off-side is defined as the other end where cylinder pressure can be arbitrarily set. The working and off-sides of the cylinder change depending on the working conditions of the robot arm. As the off-side cylinder flow changes, the working side flow must be adjusted as well to maintain the desired cylinder flow critical to precise motion control. As such, it is necessary to determine how to control the pressure in one side of the cylinder first. In the following, only the pressure control of the head-side chamber is presented; the design for the rod-end chamber can be worked out in the same way.

From (2) and (5), the head side cylinder chamber dynamics are,

$$\frac{V_1}{\beta_e} \dot{P}_1 = -A_1 \dot{x}_L + Q_{1M} + \tilde{Q}_{1M} \quad (6)$$

where x_L is the boom cylinder displacement. In order to use parameter adaptation to reduce parametric uncertainties to improve performance, it is necessary to linearly parameterize the system dynamics in terms of a set of unknown parameters θ_p . Let θ_p be $\theta_p = [\theta_{\beta_e}, \theta_Q]$, where $\theta_{\beta_e} = \frac{1}{\beta_e}$ represents the effect of unknown bulk modulus, and $\theta_Q = \tilde{Q}_{1M_o}$ represents the unknown nominal value of the flow modelling error. The cylinder dynamics for the head end chamber can be rewritten as follows.

$$\dot{P}_1 = \frac{1}{\theta_{\beta_e} V_1} (-A_1 \dot{x}_L + Q_{1M} + \theta_Q + \tilde{Q}_{1M_t}) \quad (7)$$

where $\tilde{Q}_{1M_t} = \tilde{Q}_{1M} - \theta_Q$ represents the variation of the flow modelling error with respect to its nominal value, which is assumed to be bounded by $|\tilde{Q}_{1M_t}| \leq \gamma_{Q1}$. The goal is to have the cylinder pressure P_1 regulated to a specified pressure P_{1d} . Define the pressure tracking error as

$$e_{P1} = P_1 - P_{1d} \quad (8)$$

Taking the derivative of (8) and substituting in (7)

$$\dot{e}_{P1} = \frac{1}{\theta_{\beta_e} V_1} (-A_1 \dot{x}_{2L} + Q_{1M} + \theta_Q + \tilde{Q}_{1M_t}) - \dot{P}_{1d} \quad (9)$$

If Q_{1M} is treated as a virtual control input, the pressure control law can be defined as

$$Q_{1Md} = Q_{1Mda} + Q_{1Mds} \quad (10)$$

where Q_{1Mda} is a model compensation term defined by

$$Q_{1Mda} = A_1 \dot{x}_{2L} + \hat{\theta}_{\beta_e} V_1 \dot{P}_{1d} - \hat{\theta}_Q \quad (11)$$

and Q_{1Mds} is a robust feedback term and defined as follows.

$$Q_{1Mds} = -k_p e_{P1} + Q_{1Mds2} \quad (12)$$

Q_{1Mds2} is a nonlinear robust term determined in the following. Define a positive semi-definite function V_{Ps} as

$$V_{Ps} = \frac{1}{2} \theta_{\beta_e} e_{P1}^2 \quad (13)$$

Taking the derivative of (13) using (9) with $Q_{1M} = Q_{1Md}$ the resulting equation is given by

$$\begin{aligned} \dot{V}_{Ps} &= e_{P1} \left[\frac{1}{V_1} (-A_1 \dot{x}_{2L} + Q_{1M} + \theta_Q + \tilde{Q}_{1Mt}) - \theta_{\beta e} \dot{P}_{1d} \right] \\ &= -\frac{k_{p1}}{V_1} e_{P1}^2 + e_{P1} \left[\frac{1}{V_1} (Q_{1Mds2} - \tilde{\theta}_Q - \tilde{Q}_{1Mt}) + \tilde{\theta}_{\beta e} \dot{P}_{1d} \right] \end{aligned} \quad (14)$$

Using the same technique as in [9, 12], Q_{1Mds2} can be chosen to satisfy

$$\begin{aligned} \text{i} \quad & e_{P1} \left[\frac{1}{V_1} (Q_{1Mds2} - \tilde{\theta}_Q - \tilde{Q}_{1Mt}) + \tilde{\theta}_{\beta e} \dot{P}_{1d} \right] \leq \varepsilon_p \\ \text{ii} \quad & e_{P1} Q_{1Mds2} \leq 0 \end{aligned} \quad (15)$$

where ε_p is a design parameter. To determine the adaptation law, define

$$V_{Pa} = V_{Ps} + \frac{1}{2\gamma_{\beta e}} \tilde{\theta}_{\beta e}^2 + \frac{1}{2\gamma_Q} \tilde{\theta}_Q^2 \quad (16)$$

When $\tilde{Q}_{1Mt} = 0$, noting ii of (15)

$$\dot{V}_{Pa} \leq -\frac{k_{p1}}{V_1} e_{P1}^2 + \frac{1}{\gamma_{\beta e}} \tilde{\theta}_{\beta e} \left[\dot{\hat{\theta}}_{\beta e} + \gamma_{\beta e} \dot{P}_{1d} e_{P1} \right] + \frac{1}{\gamma_Q} \tilde{\theta}_Q \left[\dot{\hat{\theta}}_Q - \frac{\gamma_Q}{V_1} e_{P1} \right] \quad (17)$$

The adaptation laws are then chosen to be

$$\begin{cases} \dot{\hat{\theta}}_{\beta e} = \text{Proj}_{\theta_{\beta e}} (-\gamma_{\beta e} \dot{P}_{1d} e_{P1}) \\ \dot{\hat{\theta}}_Q = \text{Proj}_{\theta_Q} \left(\frac{\gamma_Q}{V_1} e_{P1} \right) \end{cases} \quad (18)$$

With the above pressure control law and parameter adaptation law, using the standard ARC arguments as in [9, 12], it can be shown that a prescribed pressure transient response is achieved in general and asymptotic pressure tracking is attainable when $\tilde{Q}_{1Mt} = 0$.

3.3 Valve Level: ARC Motion Controller Design

In this subsection, an ARC motion controller is synthesized for the working chamber of the cylinder for precision motion tracking. The design is similar to those in [10, 4] and is summarized below.

Define the unknown parameter set $\theta = [\theta_1, \theta_2, \theta_3]^T$ as $\theta_1 = \frac{1}{J_c + m_L l_c^2}$, $\theta_2 = \frac{T_n}{J_c + m_L l_c^2}$, $\theta_3 = \beta_e$. The system dynamic equations can thus be linearly parameterized in terms of θ as

$$\begin{aligned} \ddot{q}_2 &= \frac{\theta_1}{J_c} \left[\frac{\partial x_L}{\partial q_2} (P_1 A_1 - P_2 A_2) - G_c(q_2) \right] + \frac{\theta_1}{l_c^2} g l_g - \frac{1}{l_c^2} g l_g + \theta_2 + \tilde{T} \\ \dot{P}_1 &= \frac{\theta_3}{V_1(q_2)} (-A_1 \frac{\partial x_L}{\partial q_2} \dot{q}_2 + Q_{1M} + \tilde{Q}_{1M}) \\ \dot{P}_2 &= \frac{\theta_3}{V_2(q_2)} (A_2 \frac{\partial x_L}{\partial q_2} \dot{q}_2 - Q_{2M} - \tilde{Q}_{2M}) \end{aligned} \quad (19)$$

where $\tilde{T} = \frac{T_d - T_{dn}}{J_c + m_L l_c^2}$. The unknown parameters $\theta_1, \theta_2, \theta_3$ and the uncertain nonlinearities, \tilde{T} , are physically bounded. In addition, it is assumed that

$$|\tilde{Q}_{1M}(x_v, \Delta P_1)| \leq \delta_{Q1}(\Delta P_1), \quad |\tilde{Q}_{2M}(x_v, \Delta P_2)| \leq \delta_{Q2}(\Delta P_2) \quad (20)$$

where $\delta_{Q1}(\Delta P_1)$, and $\delta_{Q2}(\Delta P_2)$ are known. For simplicity, let \hat{q}_2 represent the calculable part of \ddot{q}_2 , which is given by

$$\hat{q}_2 = \frac{\theta_1}{J_c} \left[\frac{\partial x_L}{\partial q_2} (P_1 A_1 - P_2 A_2) - G_c \right] + \frac{\theta_1}{l_c^2} g l_g - \frac{1}{l_c^2} g l_g + \hat{\theta}_2 \quad (21)$$

Define a switching-function-like quantity as

$$z_2 = \dot{z}_1 + k_1 z_1 = \dot{q}_2 - \dot{q}_{2r}, \quad \dot{q}_{2r} \triangleq \dot{q}_{2d} - k_1 z_1 \quad (22)$$

where $z_1 = q_2 - q_{2d}(t)$ is the output tracking error with $q_{2d}(t)$ being the reference trajectory. Differentiating (22) and noting (19)

$$\dot{z}_2 = \frac{\theta_1}{J_c} \left[\frac{\partial x_L}{\partial q_2} (P_1 A_1 - P_2 A_2) - G_c \right] + \frac{1}{l_c^2} \theta_1 g l_g - \frac{1}{l_c^2} g l_g + \theta_2 + \tilde{T} - \dot{q}_{2r} \quad (23)$$

where $\dot{q}_{2r} = \ddot{q}_{2d} - k_1 \dot{z}_1$ is calculable. In (23), define the load force as $P_L = P_1 A_1 - P_2 A_2$. If we treat P_L as the virtual control input to (23), we can synthesize a virtual control law P_{Ld} for P_L such that z_2 is as small as possible. The design details are similar to those in [10, 4] and omitted. The resulting control function P_{Ld} consists of two parts given by

$$\begin{aligned} P_{Ld}(q_2, \dot{q}_2, \hat{\theta}_1, \hat{\theta}_2, t) &= P_{Lda} + P_{Lds} \\ P_{Lda} &= \frac{\partial q_2}{\partial x_L} \left[G_c(q_2) + \frac{J_c}{\theta_1} \left(-\frac{\hat{\theta}_1}{l_c^2} g l_g + \frac{1}{l_c^2} g l_g - \hat{\theta}_2 + \dot{q}_{2r} \right) \right] \\ P_{Lds} &= P_{Lds1} + P_{Lds2}, \quad P_{Lds1} = -\frac{J_c}{\theta_{1min}} \frac{\partial q_2}{\partial x_L} (k_2 z_1 + k_2) z_2 \end{aligned} \quad (24)$$

in which P_{Lda} functions as an adaptive model compensation, and P_{Lds} is a robust control law with $k_2 > 0$ and k_{2s1} being a positive nonlinear control gain function to be specified later, and P_{Lds2} is chosen to satisfy the following robust performance conditions as in [10]

$$\begin{aligned} \text{i} \quad & z_2 \left[\frac{1}{J_c} \theta_1 \frac{\partial x_L}{\partial q_2} P_{Lds2} - \tilde{\theta}^T \phi_2 + \tilde{T} \right] \leq \varepsilon_2 \\ \text{ii} \quad & z_2 \frac{\partial x_L}{\partial q_2} P_{Lds2} \leq 0 \end{aligned} \quad (25)$$

where ε_2 is a design parameter. If P_L were the actual control input, the adaptation function as defined in [4] would be

$$\tau_2 = w_2 \phi_2 z_2, \quad \phi_2 \triangleq \left[\frac{1}{J_c} \left(\frac{\partial x_L}{\partial q_2} P_{Lda} - G_c \right) + \frac{1}{l_c^2} g l_g, 1, 0 \right]^T \quad (26)$$

where $w_2 > 0$ is a constant weighting factor. Let $z_3 = P_L - P_{Ld}$ denote the input discrepancy. Following similar derivations as in [10, 4], it can be shown that

$$\dot{z}_2 = \frac{\theta_1}{J_c} \frac{\partial x_L}{\partial q_2} z_3 - \frac{\theta_1}{\theta_{1min}} (k_2 + k_{2s1}) z_2 + \frac{\theta_1}{J_c} \frac{\partial x_L}{\partial q_2} P_{Lds2} - \tilde{\theta}^T \phi_2 + \tilde{T} \quad (27)$$

and the time derivative of positive semi-definite (p.s.d.) function V_2 defined by $V_2 = \frac{1}{2} w_2 z_2^2$ is

$$\begin{aligned} \dot{V}_2 &= \frac{1}{J_c} \frac{\partial x_L}{\partial q_2} w_2 \theta_1 z_2 z_3 + w_2 z_2 \left(\frac{1}{J_c} \theta_1 \frac{\partial x_L}{\partial q_2} P_{Lds2} - \tilde{\theta}^T \phi_2 + \tilde{T} \right) \\ &\quad - w_2 \frac{\theta_1}{\theta_{1min}} (k_2 + k_{2s1}) z_2^2 \end{aligned} \quad (28)$$

With the above development, an actual control flow can then be synthesized so that z_3 converges to zero or a small value with a guaranteed transient performance and accuracy. The specific control law varies depending on the cylinder function used. Specifically, for the retract resistive, extend overrunning, and extend overrunning regeneration modes, the head-end is the off-side chamber and is controlled by the ARC pressure controller presented before. The rod-end is then the working chamber and will be controlled by the ARC motion control law synthesized as follows.

For simplicity, assume that the ARC pressure controller is able to maintain the off-side chamber pressure at the desired constant pressure, i.e., $P_1 = P_{1d} = \text{constant}$, from (19),

$$\begin{aligned} \dot{z}_3 &= \dot{P}_L - \dot{P}_{Ld} \\ &= \theta_3 \left[-\frac{A_2^2}{V_2} \frac{\partial x_L}{\partial q_2} \dot{q}_2 + \left(\frac{A_2}{V_2} Q_{2M} \right) + \frac{A_2}{V_2} \tilde{Q}_2 \right] - \dot{P}_{Ldc} - \dot{P}_{Ldu} \end{aligned} \quad (29)$$

where

$$\begin{aligned} \dot{P}_{Ldc} &= \frac{\partial P_{Ld}}{\partial q_2} \dot{q}_2 + \frac{\partial P_{Ld}}{\partial \dot{q}_2} \ddot{q}_2 + \frac{\partial P_{Ld}}{\partial t} \\ \dot{P}_{Ldu} &= \frac{\partial P_{Ld}}{\partial \dot{q}_2} \left[-\frac{1}{J_c} \left(\frac{\partial x_L}{\partial q_2} P_L - G_c(q_2) \right) \tilde{\theta}_1 - \frac{1}{l_g} g l_g(q_2) \tilde{\theta}_1 - \tilde{\theta}_2 + \tilde{T} \right] + \frac{\partial P_{Ld}}{\partial \theta} \dot{\theta} \end{aligned} \quad (30)$$

In (30), \dot{P}_{Ldc} is calculable and can be used in the construction of control functions, but \dot{P}_{Ldu} cannot due to various uncertainties. Therefore, \dot{P}_{Ldu} has to be dealt with via certain robust feedback in this step design. Define the Q_{2L} and \tilde{Q}_2 as

$$Q_{2L} = \frac{A_2}{V_2} Q_{2M}, \quad \tilde{Q}_2 = \frac{A_2}{V_2} \tilde{Q}_2 \quad (31)$$

Then, in viewing (29), Q_{2L} can be thought as the virtual control input for (29) and step 2 is to synthesize a control function Q_{2Ld} for Q_{2L} such that P_L tracks the desired control function P_{Ld} synthesized in Step 1 with a guaranteed transient performance.

Consider the augmented p.s.d. function $V_3 = V_2 + \frac{1}{2} w_3 z_3^2$, where $w_3 > 0$ is a weighting factor. From (29)

$$\begin{aligned} \dot{V}_3 &= \dot{V}_2 + w_3 z_3 \dot{z}_3 = \dot{V}_2 |_{P_{Ld}} \\ &+ w_3 z_3 \left[\theta_3 Q_{2L} + Q_{2Lde} - \phi_3^T \tilde{\theta} + \theta_3 \tilde{Q}_2 - \frac{\partial P_{Ld}}{\partial \dot{q}_2} \tilde{T} - \frac{\partial P_{Ld}}{\partial \theta} \dot{\theta} \right] \end{aligned} \quad (32)$$

where $\dot{V}_2 |_{P_{Ld}}$ is a short-hand notation used to represent \dot{V}_2 when $P_L = P_{Ld}$ (or $z_3 = 0$), i.e. $\dot{V}_2 |_{P_{Ld}} = \dot{V}_2 - \frac{\theta_1}{J_c} \frac{\partial x_L}{\partial q_2} w_2 z_2 z_3$, and Q_{2Lde} and ϕ_3 are defined by

$$\begin{aligned} Q_{2Lde} &= \frac{1}{J_c} \frac{w_2}{w_3} \frac{\partial x_L}{\partial q_2} z_2 \tilde{\theta}_1 - \tilde{\theta}_3 \frac{A_2^2}{V_2} \frac{\partial x_L}{\partial q_2} \dot{q}_2 - \dot{P}_{Ldc} \\ \phi_3 &= \begin{bmatrix} \frac{w_2}{w_3 J_c} \frac{\partial x_L}{\partial q_2} z_2 - \frac{\partial P_{Ld}}{\partial \dot{q}_2} \left[\frac{1}{J_c} \left(\frac{\partial x_L}{\partial q_2} P_L - G_c(q_2) \right) + \frac{1}{l_g} g l_g \right] \\ - \frac{\partial P_{Ld}}{\partial \dot{q}_2} \\ - \frac{A_2^2}{V_2} \frac{\partial x_L}{\partial q_2} \dot{q}_2 + Q_{2Lda} \end{bmatrix} \end{aligned} \quad (33)$$

Similar to (24), the control function Q_{2Ld} consists of two parts given by

$$\begin{aligned} Q_{2Ld}(q_2, \dot{q}_2, P_1, P_2, \hat{\theta}, t) &= Q_{2Lda} + Q_{2Lds} \\ Q_{2Lda} &= -\frac{1}{\theta_3} Q_{2Lde} \\ Q_{2Lds} &= Q_{2Lds1} + Q_{2Lds2}, \quad Q_{2Lds1} = -\frac{1}{\theta_{3min}} (k_3 + k_{3s1}) z_3 \end{aligned} \quad (34)$$

where $k_3 > 0$ and k_{3s1} is a positive definite control gain function which will be specified later. Substitute (34) into (32) and noting (33), the time derivative of V_3 can be expressed by

$$\begin{aligned} \dot{V}_3 &= \dot{V}_2 |_{P_{Ld}} + w_3 z_3 (\theta_3 Q_{2Lds2} - \tilde{\theta}^T \phi_3 + \theta_3 \tilde{Q}_2 - \frac{\partial P_{Ld}}{\partial \dot{q}_2} \tilde{T}) \\ &- w_3 \frac{\theta_3}{\theta_{3min}} (k_3 + k_{3s1}) z_3^2 - w_3 z_3 \frac{\partial P_{Ld}}{\partial \theta} \dot{\theta} \end{aligned} \quad (35)$$

Like (25), Q_{2Lds2} is a robust control function satisfying the following two conditions

$$\begin{aligned} \text{i} \quad & z_3 \left[\theta_3 Q_{2Lds2} + \theta_3 \tilde{Q}_2 - \tilde{\theta}^T \phi_3 - \frac{\partial P_{Ld}}{\partial \dot{q}_2} \tilde{T} \right] \leq \varepsilon_3 \\ \text{ii} \quad & z_3 Q_{2Lds2} \leq 0 \end{aligned} \quad (36)$$

where ε_3 is a design parameter.

Once the control functions Q_{1Md} for Q_{1M} and Q_{2Ld} for Q_{2L} are synthesized as given in (10 and (34), the next step is to use the pressure compensated inverse valve mappings to back out the specific valve openings needed to provide the desired "flows", Q_{1Md} and Q_{2Ld} . The details can be worked out easily and are omitted.

4 Experimental Results

The completed controller is implemented on the hydraulic system shown in Fig.2. A simple extend, stop, retract and stop point to point trajectory, which represents the mostly encountered industrial operations, is used with and without a 50 pound external loading. The experimental results with and without a 50 lb. load, Fig. 3 and Fig. 4, show that the controller performs reasonable well in each case with a maximum error of 0.04 rad or approximately 2.3°. The cylinder pressures in both cases remain very low, thus achieves significant energy saving. The energy usage is calculated as the pump flow times the pressure drop from pump to tank. The energy usage is zero when the cylinder is the retracting over-running regeneration function, as seen between the time of 5.5-8.5 seconds. The plot of the energy usage includes an additional line representing the potential decrease in energy usage with a load sensing pump as seen in the simulation results. The plot of the energy usage includes an additional line representing the potential decrease in energy usage with a load sensing pump. The current set up makes use of a constant pressure supply pump that is not ideal for energy saving. A load sensing pump that can provide the needed flow at the highest working pressure would significantly reduce the energy usage if used in conjunction with the proposed programmable valve. The plot labelled as 'LS Energy Usage', calculates the anticipated energy usage if a load sensing pump was used, assuming that the pump would track the highest working pressure and add an additional 500KPa margin of pressure.

5 Conclusions

The utilization of the programmable valve and the incorporation of an ARC pressure controller and an ARC motion controller as detailed in this paper result in significant gains in energy saving while achieving cylinder motion tracking. Simulation and experimental results obtained verify the claims.

References

- [1] J. A. Aardema and D. W. Koehler. System and method for controlling an independent metering valve. *United States Patent*, (5,947,140), 1999.
- [2] Ruth Book and Carrol E. Goering. Programmable electro-hydraulic valve. In *SAE paper*, pages 28–34, Vol.1, No.2, 1999.
- [3] F. Bu and Bin Yao. Adaptive robust precision motion control of single-rod hydraulic actuators with time-varying unknown inertia : a case study. In *ASME International Mechanical Engineering*

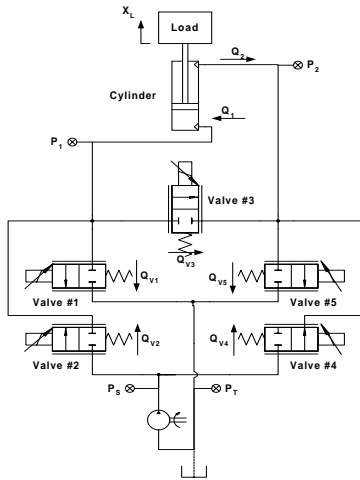


Figure 1: Programmable Valve Layout

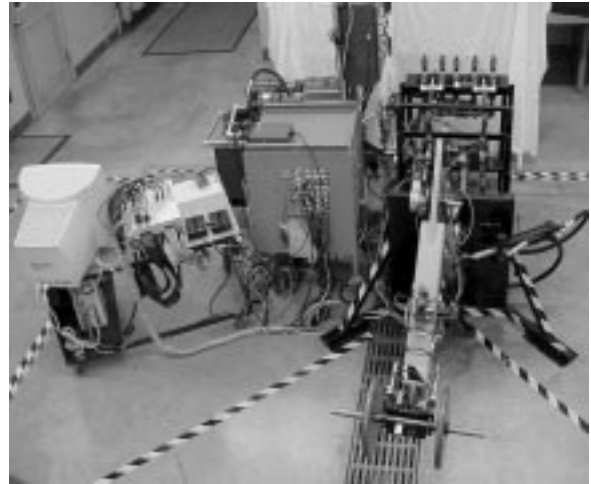


Figure 2: Experimental Setup

Congress and Exposition (IMECE), FPST-Vol.6., pages 131–138, Nashville, TN, 1999.

[4] F. Bu and Bin Yao. Nonlinear adaptive robust control of hydraulic actuators regulated by proportional directional control valves with deadband and nonlinear flow gain coefficients. In *Proc. of American Control Conference*, pages 4129–4133, Chicago, 2000.

[5] K. D. Garnjost. Energy-conserving regenerative-flow valves for hydraulic servomotors. *United States Patent*, (4,840,111), 1989.

[6] Arne Jansson and Jan-Ove Palmberg. Separate controls of meter-in and meter-out orifices in mobile hydraulic systems. *SAE Transactions*, 99(Sect 2):377–383, 1990.

[7] K. D. Kramer and E. H. Fletcher. Electrohydraulic valve system. *United States Patent*, (Re. 33,846), 1990.

[8] H. E. Merritt. *Hydraulic control systems*. Wiley, New York, 1967.

[9] Bin Yao. High performance adaptive robust control of nonlinear systems: a general framework and new schemes. In *Proc. of IEEE Conference on Decision and Control*, pages 2489–2494, San Diego, 1997.

[10] Bin Yao, F. Bu, J. Reedy, and G.T.C. Chiu. Adaptive robust control of single-rod hydraulic actuators: theory and experiments. *IEEE/ASME Trans. on Mechatronics*, 5(1):79–91, 2000.

[11] Bin Yao and M. Tomizuka. Adaptive robust control of SISO nonlinear systems in a semi-strict feedback form. *Automatica*, 33(5):893–900, 1997. (Part of the paper appeared in Proc. of 1995 American Control Conference, pp2500-2505, Seattle).

[12] Bin Yao and M. Tomizuka. Adaptive robust control of MIMO nonlinear systems in semi-strict feedback forms. *Automatica*, 37(9):1305–1321, 2001. Parts of the paper were presented in the *IEEE Conf. on Decision and Control*, pp2346-2351, 1995, and the *IFAC World Congress*, Vol. F, pp335- 340, 1996.

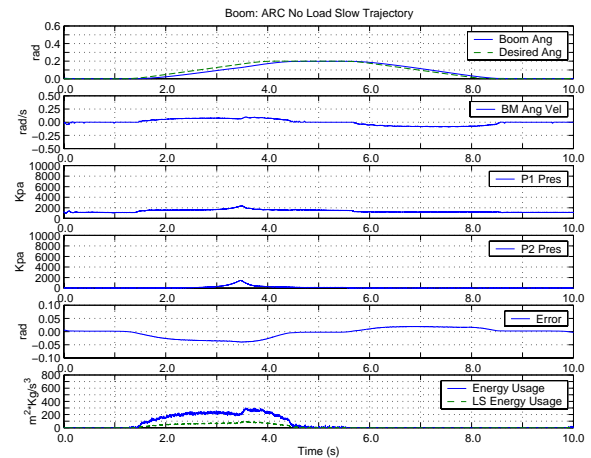


Figure 3: Boom ARC Experiment (No Load)

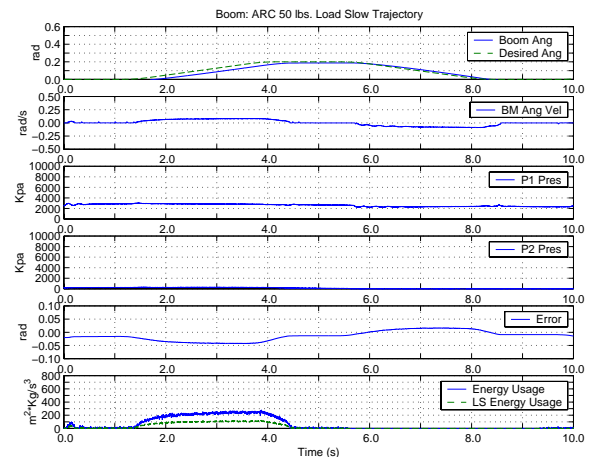


Figure 4: Boom ARC Experiment (50 lb Load)